LEOPARD syndrome-associated SHP2 mutation confers leanness and protection from diet-induced obesity

Mylène Tajan[a,b], Aurélie Batut[a,b], Thomas Cadoudal[a,b], Simon Deleruyelle[a,b], Sophie Le Gonidec[a,b], Céline Saint Laurent[a,b], Maëlle Vomscheid[a,b], Estelle Wanecq[a,b], Karine Tréguer[a,b], Audrey De Rocca Serra-Nédélec[a,b], Claire Vinel[a,b], Marie-Adeline Marques[a,b], Joffrey Pozzo[c], Oksana Kunduzova[a,b], Jean-Pierre Salles[d], Maithé Tauber[d], Patrick Raynal[e], Hélène Cavé[f], Thomas Edouard[d], Philippe Valet[a,b], and Armelle Yart[a,b,1]

[a]Institut National de la Santé et de la Recherche Médicale, U1048, F-31432 Toulouse, France; [b]Institut des Maladies Métaboliques et Cardiovasculaires, Université de Toulouse, Université Paul Sabatier, F-31432 Toulouse, France; [c]Cardiology Unit, University Hospital Center of Rangueil Toulouse, F-31432 Toulouse, France; [d]Endocrine, Bone Diseases, and Genetics Unit, Children's Hospital, University Hospital Center of Purpan Toulouse, F-31024 Toulouse, France; [e]EA4568 Laboratoire Mécanismes des Cardiopathies et Résistances Hormonales dans le Syndrome de Noonan et les Syndromes Apparentés, Université de Toulouse, Université Paul Sabatier, F-31062 Toulouse, France; and [f]Institut National de la Santé et de la Recherche Médicale Unité Mixte de Recherche S1131, Unité de Formation et de Recherche de Médecine Paris-Diderot-Institut Universitaire d'Hématologie Département de Génétique, Unité Fonctionnelle de Génétique Moléculaire Hôpital Robert Debré, F-75019 Paris, France

Edited by J. G. Seidman, Harvard Medical School, Boston, MA, and approved September 8, 2014 (received for review April 2, 2014)

LEOPARD syndrome (multiple Lentigines, Electrocardiographic conduction abnormalities, Ocular hypertelorism, Pulmonary stenosis, Abnormal genitalia, Retardation of growth, sensorineural Deafness; LS), also called Noonan syndrome with multiple lentigines (NSML), is a rare autosomal dominant disorder associating various developmental defects, notably cardiopathies, dysmorphism, and short stature. It is mainly caused by mutations of the *PTPN11* gene that catalytically inactivate the tyrosine phosphatase SHP2 (Src-homology 2 domain-containing phosphatase 2). Besides its pleiotropic roles during development, SHP2 plays key functions in energetic metabolism regulation. However, the metabolic outcomes of LS mutations have never been examined. Therefore, we performed an extensive metabolic exploration of an original LS mouse model, expressing the T468M mutation of SHP2, frequently borne by LS patients. Our results reveal that, besides expected symptoms, LS animals display a strong reduction of adiposity and resistance to diet-induced obesity, associated with overall better metabolic profile. We provide evidence that LS mutant expression impairs adipogenesis, triggers energy expenditure, and enhances insulin signaling, three features that can contribute to the lean phenotype of LS mice. Interestingly, chronic treatment of LS mice with low doses of MEK inhibitor, but not rapamycin, resulted in weight and adiposity gains. Importantly, preliminary data in a French cohort of LS patients suggests that most of them have lower-than-average body mass index, associated, for tested patients, with reduced adiposity. Altogether, these findings unravel previously unidentified characteristics for LS, which could represent a metabolic benefit for patients, but may also participate to the development or worsening of some traits of the disease. Beyond LS, they also highlight a protective role of SHP2 global LS-mimicking modulation toward the development of obesity and associated disorders.

rasopathies | ras/MAPK | energy metabolism | adipose tissue

LEOPARD syndrome (multiple Lentigines, Electrocardiographic conduction abnormalities, Ocular hypertelorism, Pulmonary stenosis, Abnormal genitalia, Retardation of growth, sensorineural Deafness) (MIM 151100) (LS), also named Noonan syndrome with multiple lentigines (NSML), is a rare autosomal dominant developmental disorder characterized by a phenotypic triad associating heart defects, facial dysmorphism, and short stature, as well as defining traits, including lentigines and deafness. With related diseases sharing all or some of these symptoms (Noonan, Costello, cardio-facio-cutaneous syndromes, neurofibromatosis type I), it belongs to the family of Rasopathies, named after the mutated genes encoding actors of the Ras/mitogen-activated protein kinases (MAPK) signaling cascade (1).

More than 80% of patients with LS heterozygously carry a missense mutation in the *PTPN11* gene, encoding the ubiquitous tyrosine phosphatase SHP2 (Src-homology 2 domain-containing phosphatase 2) (2). SHP2 plays pivotal roles in development, as revealed by embryonic lethality and gastrulation defects of its total inactivation in various organisms (worm, fly, and mice), and by the impact of its targeted deletion on the development or function of many organs (brain, heart, and lung) (3). Genetic and functional evidences have pinpointed that these effects are linked to SHP2's roles in transducing signaling fluxes in response to many growth factors/hormones. Indeed, by dephosphorylating specific tyrosine residues, it regulates key intracellular signaling pathways [Ras/MAPK, phosphoinositide-3 kinases (PI3K)/Akt, target of rapamycin (TOR) kinase, Src family kinase (SFK), Rho GTPases, S6 kinase (S6K), and JAK/STAT pathway] to adapt cell fate to variations of the environment (proliferation, migration, and metabolism) (4–9).

Central to the understanding of LS pathophysiology has been to determine the outcomes of LS-causing SHP2 mutations. Biochemical studies have revealed that LS-associated mutations result in the reduction of SHP2's catalytic activity (10–12). On

Significance

LEOPARD syndrome (multiple Lentigines, Electrocardiographic conduction abnormalities, Ocular hypertelorism, Pulmonary stenosis, Abnormal genitalia, Retardation of growth, sensorineural Deafness; LS) is a rare genetic disease associating various developmental defects mainly caused by inactivating mutations of the tyrosine phosphatase SHP2 (Src-homology 2 domain-containing phosphatase 2). SHP2 is a key regulator of essential signaling pathways (MAPK, PI3K), which confer on SHP2 major roles in development and metabolism control. However, nothing is known about the metabolic status of LS. We thus performed an extensive metabolic exploration of an original LS mouse model. These mice display a lean phenotype (reduced adiposity, improved carbohydrate metabolism), translating into resistance to obesity and associated disorders upon obesogenic diet. This phenotype correlated with defective adipogenesis, better insulin signaling, and enhanced energy expenditure and was partially corrected by MAPK inhibition. Preliminary data in LS patients are in agreement with these findings.

Author contributions: M. Tajan, P.R., H.C., T.E., P.V., and A.Y. designed research; M. Tajan, A.B., T.C., S.D., S.L.G., C.S.L., M.V., E.W., K.T., C.V., M.-A.M., J.P., and A.Y. performed research; A.D.R.S.-N., J.-P.S., M. Tauber, and H.C. contributed new reagents/analytic tools; M. Tajan, T.C., S.L.G., O.K., T.E., P.V., and A.Y. analyzed data; and M. Tajan, T.E., P.V., and A.Y. wrote the paper.

The authors declare no conflict of interest.

This article is a PNAS Direct Submission.

[1]To whom correspondence should be addressed. Email: armelle.yart@inserm.fr.

This article contains supporting information online at www.pnas.org/lookup/suppl/doi:10.1073/pnas.1406107111/-/DCSupplemental.

a functional point of view, although it has been reported that LS mutants display a dominant negative activity on Ras/MAPK activation (12, 13), other studies have demonstrated that LS-associated mutations can up-regulate this same pathway, through mechanisms that remain elusive to date (14–16). Whether LS mutants-triggered MAPK dysregulation participates in the development of the disease is unknown, and MAPK-independent events have been recently implicated in LS pathogenesis. First, phosphatase-independent regulation of p53-dependent apoptosis has been proposed to drive some aspects of LS (17). Second, we and other have recently shown that dysregulation of the PI3K pathway is causally linked to the pathophysiology of LS: Indeed, LS mutants can induce PI3K hyperactivation, thereby promoting a hypertrophic phenotype in cardiomyocytes in vitro (18). Furthermore, with using the first mouse model of LS, carrying the Y279C mutation (*Ptpn11*$^{Y279C/+}$ mice), Marin et al. nicely demonstrated that the PI3K/mTOR pathway was hyperactivated, and that rapamycin-mediated mTOR inhibition could alleviate the hypertrophic cardiomyopathy (HCM) developed by these mice (13). These data were confirmed in transgenic mice overexpressing in the cardiomyocyte another LS mutant of SHP2 (Q510E mutation), which could recover from their HCM upon rapamycin treatment (19). However, whether PI3K/mTOR hyperactivation is responsible for other traits of the disease, and whether other signaling dysfunctions are involved in LS ontology, remain to be established.

In addition to its pleiotropic roles in development, SHP2 also plays key functions in homeostasis maintenance, notably by regulating energetic metabolism. Indeed, although an initial study using hemizygous *Ptpn11*$^{+/-}$ mice did not reveal any obvious metabolic phenotype, transgenic mice expressing a dominant negative mutant of SHP2 have been shown to exhibit impaired glucose homeostasis (20, 21). Moreover, different studies using tissue-specific knockouts have highlighted SHP2 involvement in metabolism regulation. Indeed, SHP2 plays a key role in leptin sensitivity in neurons and in central energy balance control (22–24). Moreover, in muscle and in liver, SHP2 appears to differently modulate insulin sensitivity, although it also promotes insulin biosynthesis in the pancreas, uncovering a complex role of SHP2 in tuning glucose homeostasis (25-28). Finally, recent studies have revealed a potential, albeit controversial, role for SHP2 in regulating adipogenesis in vitro and in vivo (29–31).

These critical impacts of SHP2 loss of function in multiple aspects of metabolism regulation infer that its dysregulation in LS can give rise to metabolic perturbations, which could have significant consequences for the patients. However, the metabolic status associated with LS has not been explored to date. In the present study, we took advantage of an original knock-in mouse model, carrying the common LS-associated, T468M, mutation of SHP2, to perform an extensive metabolic exploration. We clearly showed that these mice have reduced adiposity and increased energy expenditure, associated with improved overall metabolic profile, resulting in resistance to diet-induced obesity (DIO) and associated-adverse effects when challenged with high fat diet (HFD). Moreover, chronic treatment of LS mice with low doses of MEK inhibitor, but not with rapamycin, resulted in weight gain and increase in adiposity, whereas both treatments decreased glucose tolerance. Interestingly, preliminary data provide first evidence, to our knowledge, that patients with LS may display a similar phenotypic trait.

Results

***Ptpn11*$^{T468M/+}$ Mouse Model Recapitulates LS Features.** To explore the global outcomes of LS-causing SHP2 mutations, we generated a knock-in mouse model carrying the T468M mutation, one of the two most frequent SHP2 mutations borne by LS patients (Fig. 1*A* and Fig. S1). We first performed a general phenotyping of the *Ptpn11*$^{T468M/+}$ mouse model to assess whether this strain recapitulated the features of LS. *Ptpn11*$^{T468M/+}$ mice exhibited a slight growth and weight retardation compared with their WT littermates (Fig. S2*A*), as already observed in another LS mouse model (13). Computed tomography analysis revealed reduced skull length, increased interorbital distance, and significantly increased skull width-to-length ratio, indicating that *Ptpn11*$^{T468M/+}$ mice showed signs of craniofacial abnormalities (Fig. S2*B* and Table S1). Strikingly, *Ptpn11*$^{T468M/+}$ mice also display splenomegaly (Fig. S2*C*), a feature that was not found in a small cohort of *Ptpn11*$^{Y279C/+}$ animals (13). Moreover, these animals had significantly reduced blood pressure, coming with decreased pulse height and heart rate (Fig. S2 *D–F*). Regarding cardiac function, 30-wk-old *Ptpn11*$^{T468M/+}$ mice exhibited a significant increase in heart/body ratio compared with WT mice (Fig. S2*G*). Subsequent assessment of left ventricular function using M-mode

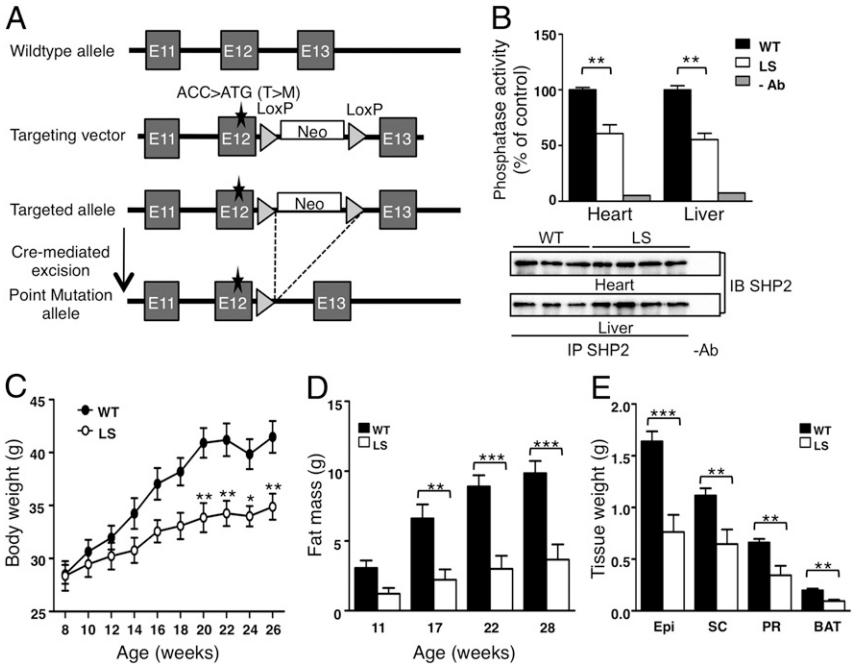

Fig. 1. LS mice display reduced body mass and adiposity. (*A*) Schematic representation of the homologous recombination strategy. (*B*) SHP2 was immunoprecipitated from heart and liver extracts of WT and LS mice (3–4 animals per group), and then a phosphatase assay was conducted by using phospho-Src peptide as a substrate. A control without antibody was also performed (-Ab) (**$P < 0.01$, unpaired two-tailed Student *t* test). (*Lower*) Quality and specificity of immunoprecipitations were verified by Western blot. (*C–E*) WT ($n = 8$) and LS ($n = 6$) animals were fed a normal diet. At indicated ages, they were weighted (*C*) or placed in an EchoMRI apparatus to determine fat mass (*D*) (*$P < 0.05$; **$P <$ 0.01, ***$P < 0.001$, two-way ANOVA plus Bonferroni post hoc test). At 30 wk of age, animals were euthanized, and then their fat pads were weighted (BAT, brown adipose tissue; Epi, epididymal; PR, perirenal; SC, s.c.) (**$P < 0.01$, ***$P < 0.001$, unpaired two-tailed Student *t* test) (*E*).

echocardiography revealed an increase in left ventricular internal diameter in *Ptpn11*$^{T468M/+}$ animals and thinning of their intraventricular septum and left ventricular posterior wall, two features evoking dilated cardiomyopathy (DCM) (Table S2). At the functional level, hearts from *Ptpn11*$^{T468M/+}$ animals display cardiac dysfunction, as shown by reduced stroke volume and proportional decrease in fractional shortening (FS) and ejection fraction (EF). Younger, 15-wk-old, LS mice, displayed enlargement of the left ventricle, revealing early stage of hypertrophy, suggesting that *Ptpn11*$^{T468M/+}$ mice develop a HCM that evolves to DCM, as reported in another LS mouse model (13). Moreover, analysis of insulin-evoked signaling in heart extracts showed increased Akt phosphorylation and decreased Erk1/2 phosphorylation (Fig. S2*H*), as previously observed in *Ptpn11*$^{Y279C/+}$ mice (13). Thus, this *Ptpn11*$^{T468M/+}$ mouse model recapitulates the main features of LS, in particular growth retardation, craniofacial abnormalities, and cardiomyopathy. Thereafter, *Ptpn11*$^{T468M/+}$ mice will be referred to as LS animals.

Because LS-causing SHP2 mutations have been shown to inactivate SHP2's phosphatase activity in vitro (10, 11, 18), we next assessed the impact of the T468M mutation in vivo. To this aim, SHP2 was immunoprecipitated from heart and liver extracts, and phosphatase assays were performed by using standard phosphotyrosine substrate. As shown in Fig. 1*B*, phosphatase activity was reduced by one-half in tissues from LS mice compared with WT animals. Thus, this result shows that the heterozygous expression of the T468M mutant of SHP2 translates into a 50% decrease in SHP2 activity in vivo, similarly to what was observed for another LS mutation (13).

LS Mice Display Reduced Body Weight and Adiposity. To explore the metabolic status associated with LS condition, we monitored the weight of WT and LS males. As shown in Fig. 1*C*, LS mice gained less weight than their WT littermates (16% less at 26 wk of age), despite similar food intake between genotypes [WT (n = 7): 4.97 ± 0.32 g/d; LS (n = 12): 5.43 ± 0.33 g/d, not significant, unpaired two-tailed Student t test). To further document this phenotype, we analyzed body composition at various ages. Lean mass was not different between genotypes, although the size of some organs was significantly reduced (Fig. S3 *A–C*), and lean mass proportion was significantly increased (Fig. S3 *D–F*), suggesting that reduced weight in LS was not primarily due to lean mass diminution. In contrast, fat mass was significantly decreased in LS mice, those animals displaying in average two-thirds less fat mass than their WT littermates (Fig. 1*D* and Fig. S3*G*). Coherently, epididymal, s.c., and perirenal white adipose tissues, and brown adipose tissue (BAT), were significantly smaller in LS animals (Fig. 1*E* and Fig. S3*H*). In line with reduced fat mass, plasma levels of insulin and leptin were significantly decreased in LS mice, leptinemia being more than fourfold reduced (Table 1). Thus, from this set of data, we conclude that systemic expression of a LS mutation of SHP2 results in leaner mice with a strong reduction of adiposity.

Impaired Adipocyte Differentiation in LS Mice. We next sought the origin of reduced adiposity in LS mice. To this aim, we determined whether LS mice-derived adipose tissue consisted of smaller and/or fewer adipocytes, by measuring the size of fat cells isolated from epididymal fat pads. As shown in Fig. 2*A*, the size distribution of adipocytes derived from LS mice revealed a depletion of the small adipocyte subpopulation for the benefit of bigger cells. Consequently, the mean diameter was significantly increased for LS adipocytes (Fig. 2*A, Inset*). Of note, adipocyte enlargement in LS mice could also participate to the reduction of adiponectin level (Table 1). Taking into account the total epididymal fat pads weights, we could estimate that adipocyte number was reduced by one-half in LS animals compared with their controls. Increased proportion of bigger adipocytes was also observed in s.c. adipose tissue (Fig. S4*A*). Thus, we conclude that LS animals have less adipocytes, in particular in their epididymal adipose tissue.

Considering the lower amount of adipocytes and the increased proportion of large adipocytes in LS mice derived-adipose tissues, we explored the possibility of impaired adipogenesis in LS mice. Indeed, a positive role for SHP2 in adipogenesis has already been identified in vitro and in vivo (29, 30). We isolated the stroma vascular fraction (SVF) from epididymal and s.c. adipose tissues of WT and LS mice and challenged the ability of SVF-derived preadipocytes to differentiate into adipocytes in vitro. The amount of refringent, lipid droplet-accumulating cells (i.e., differentiated preadipocytes) seemed reduced for LS-mice derived SVFs compared with those from WT littermates (Fig. 2*B*). Moreover, whereas expression of differentiated preadipocyte markers (*aP2*, *HSL*, *Adiponectin*) considerably rose during the differentiation process in WT cells, it was significantly delayed in LS-derived cells isolated from epididymal adipose tissue (Fig. 2*C*). Expression of those genes was mostly blocked even in SVF-derived precursors from s.c. adipose tissue (Fig. 2*D*). In addition, the expression of *PPARγ2*, a major inductor of adipocyte differentiation, was also dampened down in comparison with WT cells (Fig. 2 *C* and *D*). Thus, these data indicate that expression of a LS-associated SHP2 mutant impairs adipocyte differentiation. Furthermore, we observed that expression of the anti-adipogenic factor *Pref-1* was increased in SVF from epididymal adipose tissue (Fig. S4*B*) and that the proadipogenic factor IGF-I was significantly reduced in plasma from young LS mice (Fig. S4*C*). Altogether, these results suggest that LS condition is associated with defective adipogenesis, which could explain the reduced adiposity of LS mice.

LS Mutation Impacts Adipose Tissue Activity. Because adipose tissue amount is also the resultant of its metabolic activity, we sought changes in adipose tissue metabolism. Thus, we explored the expression level of key adipocyte metabolism-regulating genes in LS and WT mice. As shown in Fig. 3*A*, expression of lipogenesis-regulating genes (*aP2*, *SREBP1*, *FAS*) was similar between WT and LS mice. In contrast, there was a significant overexpression of two key lipases (*HSL*, *ATGL*) in the adipose tissue of LS mice, suggesting that lipolysis could be enhanced in LS adipose tissue. Supporting this view, basal glycerol release, taken as readout of lipolytic activity, was strongly increased in LS adipocytes isolated from epididymal fat pads (Fig. 3*B*). This higher rate of glycerol release was also observed in LS adipocytes at all tested doses of isoproterenol, which was probably due to increased basal lipolysis. Therefore, this finding suggests that adipose tissues in LS mice have an enhanced lipolytic activity, which could contribute to their defect in adipose tissue maintenance.

LS Condition Is Associated with a Lean, but Not Lipodystrophic, Phenotype. Given the significant reduction of fat pads in LS mice, we next assessed its consequences on whole body metabolism. Indeed, reduced adiposity can define lipodystrophy or leanness, depending on whether it associates with lipotoxicity and insulin resistance.

First, we evaluated whether global lipid metabolism was affected by the reduced amount of fat tissue. Interestingly, plasma cholesterol, triglycerides, and free fatty acids concentration were not different between genotypes (Table 1). Moreover, lipid deposits in liver and muscle were not increased in LS mice, and were even significantly reduced, as revealed by decreased triglycerides content, which came along with significantly lower plasma alanine transaminase (ALT) concentration (Table 1). Thus, this set of data suggests that LS mice can efficiently manage lipids despite their reduced adiposity.

Then, to explore carbohydrate metabolism, WT and LS animals were assayed for oral glucose tolerance test (OGTT). As shown in Fig. 4*A*, at 11 wk of age, LS mice already displayed a better glucose tolerance than their WT littermates, a difference that was even more prominent in older, 28-wk-old animals. Improved glucose tolerance in LS mice correlated with a significant reduction of their insulinemia measured before and 15 min after glucose bolus (Fig. 4*B*) and with better insulin tolerance (Fig. 4*C*)

Table 1. Metabolic parameters of 30-wk-old, fasted WT and LS mice fed a ND or a HFD

	ND		HFD	
Metabolic parameters	WT (n = 8)	LS (n = 6)	WT (n = 15)	LS (n = 13)
Plasma				
Glycemia, g/L	1.32 ± 0.09	1.15 ± 0.07	1.70 ± 0.09	1.46 ± 0.07*
Insulinemia, pg/mL	2117 ± 423	527 ± 118**	6424 ± 1611	791 ± 183*
ALT, U/L	26.38 ± 2.08	17.17 ± 1.66**	96.40 ± 15.57	39.46 ± 13.86*
AST, U/L	59.38 ± 6.05	44.33 ± 2.59	103.60 ± 9.80	61.54 ± 6.39**
Fructosamine, μmol/L	n.d.	n.d.	211.1 ± 12.4	155.4 ± 10.7*
Cholesterol, mmol/L	2.58 ± 0.19	2.48 ± 0.25	4.16 ± 0.19	3.37 ± 0.21**
Triglycerides, mmol/L	1.52 ± 0.16	1.35 ± 0.22	1.30 ± 0.15	1.32 ± 0.14
FFA, mmol/L	0.37 ± 0.02	0.46 ± 0.06	0.42 ± 0.08	0.52 ± 0.08
Leptin, ng/mL	30.55 ± 5.29	7.21 ± 3.03**	88.00 ± 9.74	36.85 ± 7.78**
Adiponectin, μg/mL	6.68 ± 0.33	5.20 ± 0.21**	5.68 ± 0.23	5.10 ± 0.31
Tissues				
Liver triglycerides, mg/g liver	63.27 ± 2.92	36.65 ± 3.74***	Fig. 6	Fig. 6
Muscle triglycerides, g/g prot	0.12 ± 0.02	0.06 ± 0.02*	Fig. 6	Fig. 6

Data represent mean ± SEM. *P < 0.05, **P < 0.01, ***P < 0.001, unpaired two-tailed Student t test. ALT, alanine transaminase; AST, aspartate transaminase; FFA, free fatty acids; n.d., not determined.

compared with WT animals. Consistent with this profile, insulin-induced glucose uptake was significantly increased in isolated adipocytes from LS mice-derived epididymal adipose tissue (Fig. 4*D*). Importantly, the doses of insulin necessary to induce glucose transport and to reach a plateau were lower in LS adipocytes, suggesting an increased insulin sensitivity of LS cells. Supporting these findings, following insulin injection, Akt and Erk1/2 phosphorylations were augmented in insulin-sensitive tissues from LS animals compared with WT mice, notably in adipose tissue (Fig. 4*E*). To determine whether this effect was a direct consequence of SHP2 mutants expression, two LS-causing SHP2 mutants (T468M, Y279C), or WT SHP2 as a control, were expressed in lieu of endogenous SHP2 into murine embryonic fibroblasts (MEF), and those cells were stimulated with insulin. Interestingly, insulin-induced Akt and Erk1/2 phosphorylations were both significantly increased in LS mutant-expressing cells, showing that expression of LS mutants into cells was sufficient to enhance insulin signaling (Fig. 4 *F* and *G*). Altogether, this result demonstrates that reduced adiposity in LS is associated with improved glucose tolerance, which can conceivably arise from enhanced insulin sensitivity, suggesting that LS mice display a lean, but not lipodystrophic, phenotype.

Chronic Treatment of LS Mice with MEK Inhibitor, but Not Rapamycin, Results in Weight and Adiposity Gain. LS mutants have been reported to affect the activation of the PI3K/Akt/mTOR and MAPK pathways in different biological systems (12–16, 18). Consistently, in our study, we observed that expression of the T468M mutant of SHP2 resulted in insulin-evoked PI3K/Akt and MAPK pathway hyperactivation in several metabolic tissues.

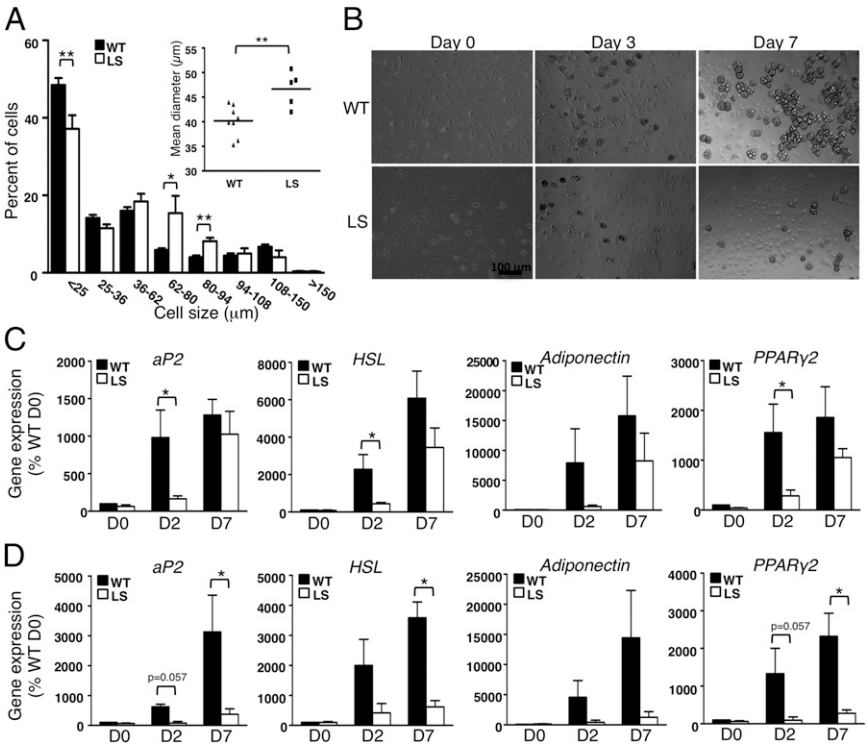

Fig. 2. Impaired adipocyte differentiation potential of LS-derived SVF cells. (*A*) Adipocytes from epididymal adipose tissue of 30-wk-old WT (n = 8) and LS (n = 6) mice were isolated and their size was determined by using a Multisizer Coulter apparatus. (*A Inset*) Mean adipocyte diameter was calculated. Individual value and mean are represented (*P < 0.05; **P < 0.01, unpaired two-tailed Student t test). (*B–D*) Six- to 8-wk-old WT and LS mice were euthanized (10 mice per group, n = 3), then their adipose tissues were withdrawn, SVF cells were purified, seeded into culture, and incubated in adipocyte differentiation medium. Representative photographs were taken at indicated times for epididymal adipose tissue-derived SVF cells (*B*). At indicated times, SVF cells derived from epididymal (*C*) or s.c. (*D*) adipose tissues were collected, then their RNAs were purified and expression of the indicated genes was determined by real-time PCR (*P < 0.05, Mann–Whitney nonparametric test).

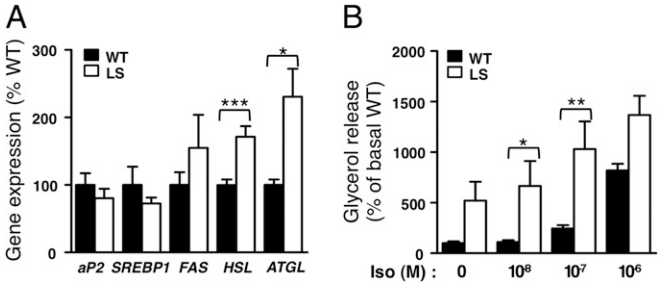

Fig. 3. Increased lipolysis in adipocytes from LS mice. Adipocytes were isolated from epididymal adipose tissue of 30-wk-old WT ($n = 8$) and LS ($n = 6$) mice. (*A*) Adipocyte RNAs were extracted, and then expression of indicated genes was determined by real-time PCR (*$P < 0.05$; ***$P < 0.001$, unpaired two-tailed Student *t* test). (*B*) Adipocyte aliquots from epididymal adipose tissue were treated with the indicated doses of isoproterenol (Iso), and released glycerol was quantified (*$P < 0.05$; **$P < 0.01$, two-way ANOVA plus Bonferroni post hoc test).

Therefore, we assessed the impact of chronic inhibition of those pathways on the metabolic phenotype of LS mice. To this aim, we treated 25-wk-old LS and WT animals for 1 mo with the mTOR inhibitor rapamycin, which has been proven to efficiently revert PI3K/Akt/mTOR hyperactivation-driven HCM in another LS mouse model (13), or with the MEK inhibitor PD0325901 (Fig. S5*A*). At the end of the treatment, PD0325901-injected mice, but not vehicle- or rapamycin-treated animals, had significantly gained weight (Fig. 5*A*). Interestingly, weight gain correlated with significant increase in adiposity for LS mice receiving MEK inhibitor, and concurrent decrease of lean mass proportion (Fig. 5 *B* and *C*). Moreover, we performed an OGTT before and after 2 wk of treatment. As shown in Fig. 5*D*, glucose tolerance, which inversely correlates with the area under glucose curve (AUC), was strongly reduced upon rapamycin and, to a lesser extent, after PD0325901 treatment, which may arise from direct, signaling-dependent, or indirect, adiposity-related effects on insulin sensitivity, respectively. After 2 wk of treatment, food intake was not significantly different among the three groups (Fig. 5*E*), whereas PD0325901-treated mice had already gained significant weight [Ctrl ($n = 5$): 102.9 ± 1.27% vs. PD ($n = 5$): 110.1 ± 1.75%, *$P < 0.05$, unpaired two-tailed Student's *t* test]. Of note, with the exception of food intake, similar results were obtained with WT animals (Fig. S5 *B–F*). Altogether, these results suggest that MAPK hyperactivation in LS mice may participate, at least in part, to the setting of their lean phenotype.

LS Mice Are Resistant to HFD-Induced Obesity and Associated Pathologies. To get further insights into the metabolic consequences of LS-associated SHP2 mutation, we then challenged LS and WT mice to HFD. Interestingly, LS mice gained much less weight than their control littermates and remained lean, whereas WT animals develop an obese phenotype (Fig. 6*A*). This lower weight gain correlated with a significant reduction of fat mass at all tested ages (Fig. 6*B* and Fig. S6*A*). Global lean mass was equivalent between genotypes, and lean mass proportion was coherently increased in LS mice (Fig. S6 *B* and *C*). Moreover, s.c., perirenal, and brown adipose tissue deposits were significantly smaller in HFD-fed LS animals, although the epididymal fat pads were not different between genotypes, which may result, at least in part, from a saturating effect in WT animals (Fig. 6*C* and Fig. S6*D*). The amount of small adipocytes was lower in adipose tissue from LS mice, evoking a defect in recruiting new adipocytes for differentiation, which could participate to their reduced fat gain (Fig. S6*E*). Noticeably, the proportion of bigger adipocytes was markedly increased in LS mice, suggesting that LS adipose tissue can, to a certain extent, compensate the reduced cell number through increased hypertrophy, which could also explain that the weight of epididymal fat pads caught up with those of WT animals. Nevertheless, lipolytic activity was still significantly enhanced in adipocytes derived from HFD-fed LS mice (Fig. S6*F*). Regarding adipose tissue secretions, leptin plasma level was much lower in LS animals, consistent with lower fat mass (Table 1). Moreover, whereas adiponectin level decreased under HFD in WT animals, it remained almost constant in LS animals. Altogether, these data reveal that LS mice are somehow resistant to HFD-induced obesity.

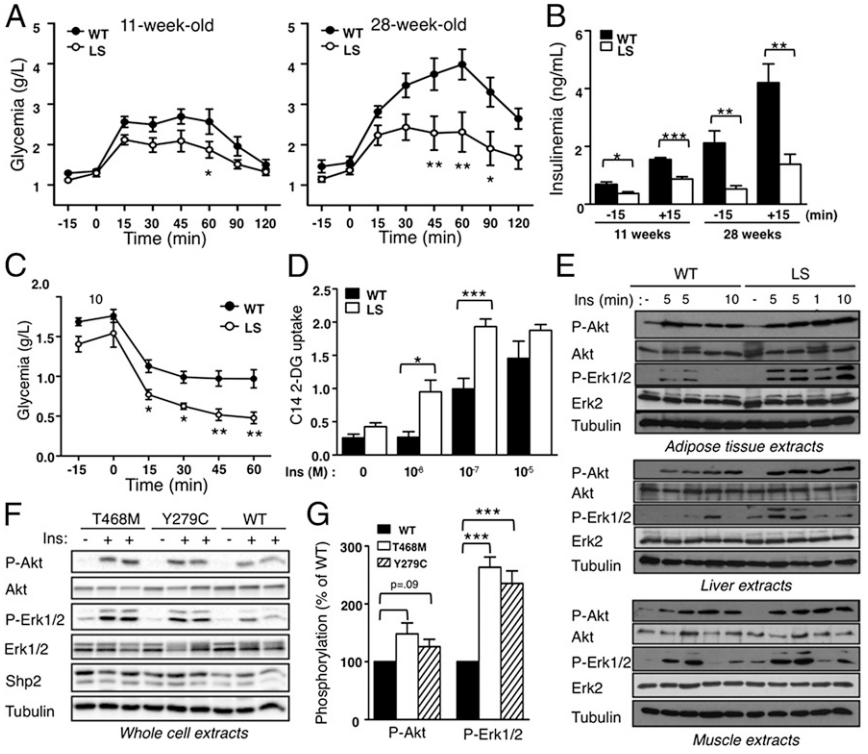

Fig. 4. Improved carbohydrate metabolism in LS mice. (*A* and *B*) At indicated ages, 6-h starved WT ($n = 8$) and LS ($n = 6$) mice were fed with 3 g/kg glucose. (*A*) Glycaemia was determined by colorimetry at indicated times (*$P < 0.05$; **$P < 0.01$, two-way ANOVA plus Bonferroni post hoc test). (*B*) Insulin levels were determined by ELISA before (–15 min) and after (+15 min) glucose load (*$P < 0.05$; **$P < 0.01$; ***$P < 0.001$, unpaired two-tailed Student *t* test). (*C*) Twenty-five–wk–old animals were injected i.p with insulin, then glycaemia was determined by using a glucometer (*$P < 0.05$; **$P < 0.01$, two-way ANOVA plus Bonferroni post hoc test). (*D*) Isolated adipocytes from 30-wk-old WT ($n = 6$) and LS ($n = 6$) mice were incubated with ^{14}C 2-deoxyglucose (C^{14} 2-DG) and stimulated or not with the indicated doses of insulin, then ^{14}C 2-DG uptake was determined (*$P < 0.05$; ***$P < 0.001$, two-way ANOVA plus Bonferroni post hoc test). (*E*) Sixteen-week-old animals were i.p. injected with 10 mU/g insulin or PBS (-) as a control, euthanized after 5 or 10 min, then their tissues were withdrawn and protein extracts were analyzed by Western blot. (*F* and *G*) MEFs expressing SHP2 WT or its LS derivatives (T468M, Y279C) were stimulated or not with insulin (Ins), then lysed and processed for Western blot (*F*). Western blots from four independent experiments were quantified with Image Lab (Bio-Rad) (*$P < 0.05$; ***$P < 0.001$, paired two-tailed Student *t* test) (*G*).

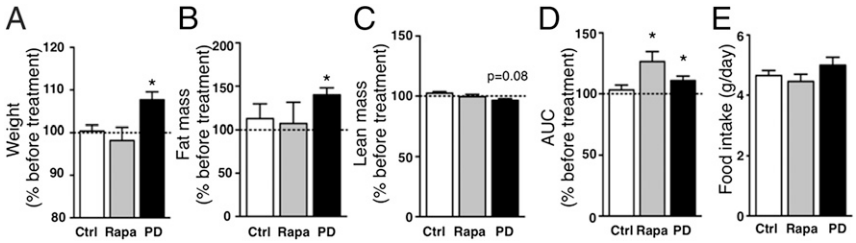

Fig. 5. Chronic MEK inhibition induces weight and adiposity gains in LS mice. LS animals were treated with vehicle (Ctrl, $n = 9$), PD0325901 (PD, 1 mg·kg^{-1}·d^{-1}, $n = 5$), or rapamycin (Rapa, 2 mg·kg^{-1}·d^{-1}, $n = 8$) for 1 mo. (*A*) Animals were weighted before and after treatment, and weight gain was calculated for each animal. (*B* and *C*) Before and after treatment, animals were placed in an EchoMRI apparatus, fat (*B*) and lean (*C*) masses were determined, and fat gain was calculated. (*D*) Animals were subjected to an OGTT before and after 2 wk of treatment, the AUC were determined, and AUC variation was calculated. Statistical significance was assessed by using a paired two-tailed Student *t* test (*$P < 0.05$). (*E*) Animals were placed in individual cages and food pellets were weighted over a 2-wk period (nonsignificant, unpaired two-tailed Student *t* test).

We next analyzed the development of obesity-associated complications in LS mice. OGTT experiments revealed that, throughout the obesogenic diet, LS mice appeared less gluco-intolerant than their control littermates (Fig. 6*D*), which was associated with lower glycaemia and decreased amount of glycated proteins (fructosamine) in plasma of LS mice (Table 1). In addition, while fasted and glucose-induced insulinemia rose in WT mice throughout the diet, they remained similar in LS mice, resulting in a marked reduction of insulin levels in LS animals compared with their control littermates (eightfold and fourfold, respectively, at the end of the HFD period) (Fig. 6*E* and Table 1). Coherently, homeostasis model assessment of insulin resistance (HOMA-IR) calculation showed that after 18 wk of HFD, LS mice remained much less resistant to insulin than their control littermates (1.25 ± 0.35 vs. 10.31 ± 2.6, *$P < 0.05$, unpaired two-tailed Student's *t* test with Welch correction). Consistent with this observation, LS mice also displayed improved insulin tolerance during insulin tolerance test (ITT) (Fig. 6*F*). Moreover, we measured a significant reduction of ALT, aspartate transaminase, and cholesterol in plasma from LS mice (Table 1) as well as of ectopic lipid deposits in liver and muscle (Fig. 6 *G–I*). Hepatic triglycerides were almost reduced by half in LS mice (Fig. 6*G*), which could contribute to their reduced liver weight (Fig. S6*G*). Altogether, these data document a protection toward obesity and its associated deleterious effects in LS mice.

Lean Phenotype Is Associated with Enhanced Energy Expenditure at the Whole Body Level. Given the lean and obesity-resistance phenotype of the LS mice, we next searched at which level the energetic equilibrium could be imbalanced in these animals. Food intake was identical for WT and LS mice, both under normal diet (ND) and HFD, excluding that this phenotype primary arose from reduced calories supply (Fig. 7*A*). Moreover, we determined that feces from WT and LS animals contained equivalent amounts of energy, suggesting that these animals do not display intestinal absorption defects (Fig. 7*B*). In addition, we did not observe significant changes in body temperature (Fig. S7*A*). We thus hypothesized that LS-associated SHP2 mutations might improve energetic substrates management. Therefore, we determined energy expenditure (EE) in WT and LS mice through an indirect calorimetry approach. Interestingly, whereas the LS mice's locomotor activity was not enhanced (Fig. 7*C*) and the respiratory quotient (RQ) was similar in both genotypes (Fig. 7*D*), EE was significantly increased in LS mice compared with their control littermates, both under ND and HFD (Fig. 7*E*). Equivalent RQ excluded major change in the fuel-partitioning patterns, suggesting that increased EE resulted from higher catabolism of both carbohydrates and lipids

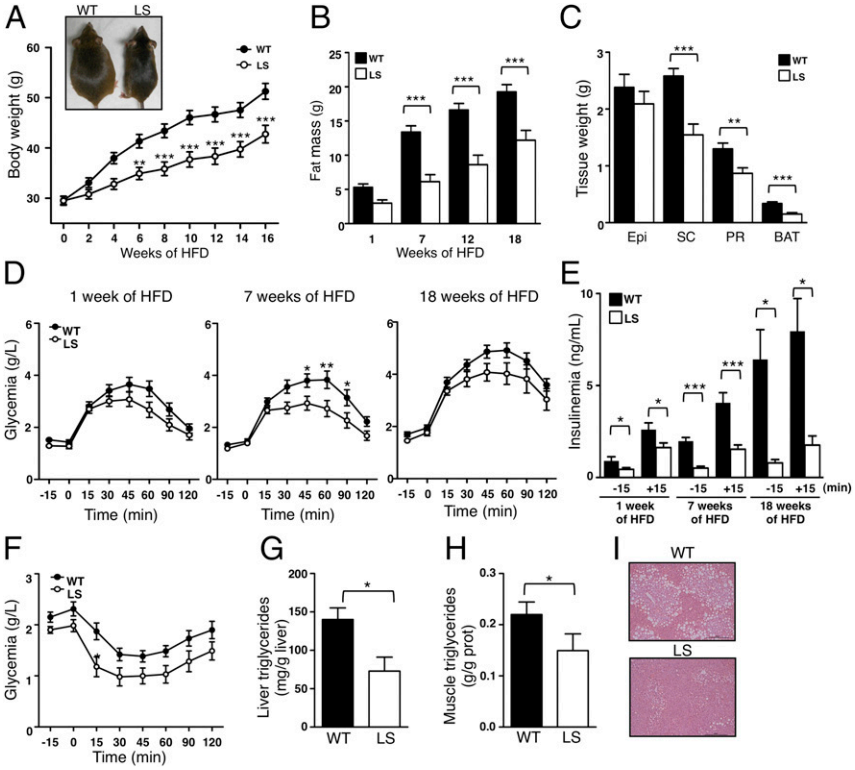

Fig. 6. LS mice are resistant to HFD-induced obesity and seem protected from obesity-associated glucointolerance, insulin resistance and ectopic lipid deposits. (*A–F*) WT ($n = 14$) and LS ($n = 13$) animals were fed a HFD, and analyses were performed as in Fig. 1 *C–E* and 4 *A–C*. (*G* and *H*) At 30 wk of age, liver (*G*) and gastrocnemius muscle (*H*) from WT and LS animals were withdrawn and triglycerides content was determined (*$P < 0.05$, Mann–Whitney nonparametric test). (*I*) Representative pictures of H&E liver sections.

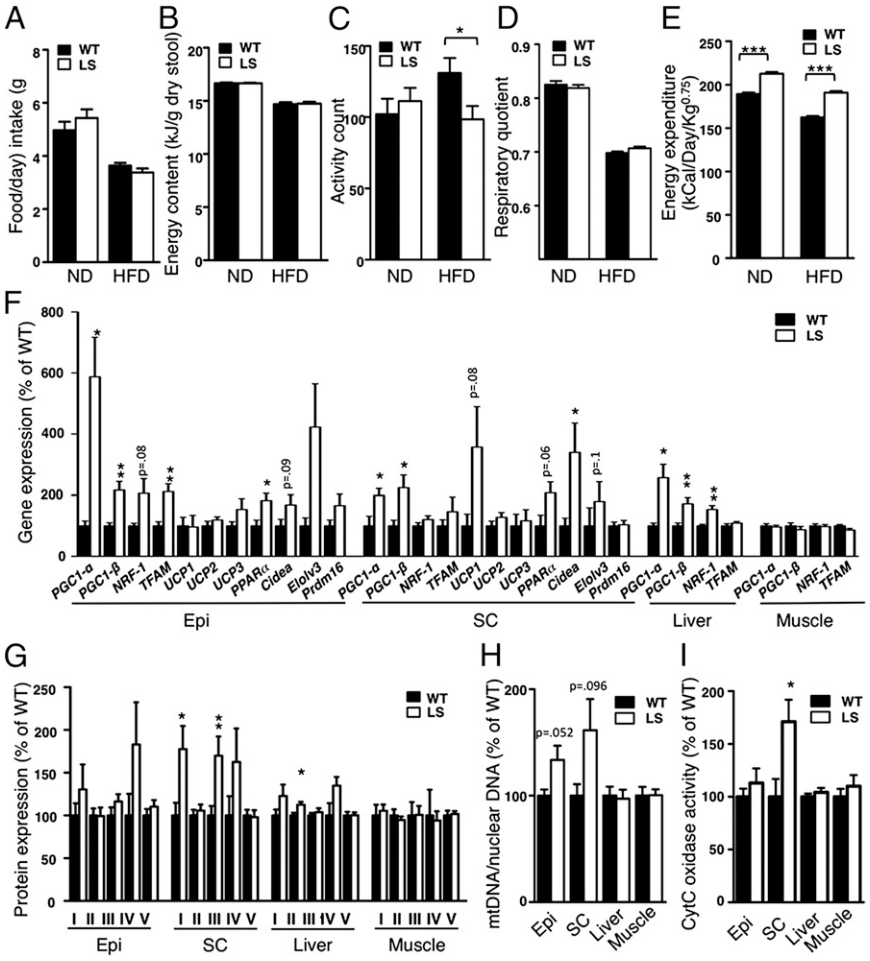

Fig. 7. Increased energy expenditure in LS animals. (*A*) Twenty-week-old WT and LS mice maintained under ND (7 WT, 12 LS) or HFD (7 WT, 6 LS) were placed in individual cages, then food pellets were regularly weighted to determine food intake (nonsignificant, unpaired two-tailed Student *t* test). (*B*) WT and LS mice maintained under ND (8 WT, 12 LS) or HFD (9 WT, 7 LS) were placed in individual cages for 3 d, then stool were collected, dried, and energy content was determined by using a bomb calorimeter (nonsignificant, unpaired two-tailed Student *t* test). (*C–E*) Sixteen- to 18-wk-old WT and LS animals maintained under ND (6 WT, 6 LS) or HFD (7 WT, 6 LS) were placed in individual chambers. After 24 h of acclimatization, they were subjected to indirect calorimetry analysis for 24 h. Activity (*C*), respiratory quotient (*D*) and energy expenditure (*E*) were determined (*$P < 0.05$; ***$P < 0.001$, two-way ANOVA with repeated measures). (*F–I*) Adipose tissues, liver, and muscle samples from 30-wk-old WT and LS mice (8 WT, 8 LS) were processed for real-time PCR analysis to determine expression of the indicated genes (*F*), for Western blot analysis to assess expression of respiratory chain complexes I to V (*G*), for determination of mitochondrial DNA content (*H*) and for cytochrome C activity from tissues homogenates (*I*) (*$P < 0.05$; **$P < 0.01$, unpaired two-tailed Student *t* test).

in LS animals. Thus, these results infer that decreased body weight and adiposity in LS mice can be due to increased metabolic rate.

To get insights into the origin of increased EE, we then analyzed the expression pattern of a series of genes involved in mitochondria biogenesis and function. Interestingly, both *PGC-1*α and β were overexpressed in epididymal and s.c. adipose tissues from LS mice fed a ND (Fig. 7*F*), and *PGC-1*α overexpression was found in all fat pads tested (Fig. S7*B*). Moreover, expression of two PGC-1–target genes involved in mitochondriogenesis, *TFAM* and *NRF-1*, was also increased in epididymal adipose tissue, whereas the expression of *UCP1* gene was augmented in s.c. adipose tissue from LS mice. Importantly, expression of several markers of adipose tissue "beiging" (*PPARα, Cidea, Elolv3*) was enhanced in adipose tissues from LS mice. Of note, up-regulation of *PGC-1*α, *PGC-1*β and *NRF-1* was also found in liver from LS mice compared with WT animals, whereas we did not observe any change in muscle (Fig. 7*F*). In line with a possible increase in mitochondria amount and/or function, Western blot analysis of mitochondrial complexes revealed a slight up-regulation of several of these proteins in tissues from LS mice, notably in adipose tissues and liver (Fig. 7*G*). Moreover, quantification of mitochondrial DNA revealed a upward trend for mitochondria density in epididymal and s.c. adipose tissues (Fig. 7*H*) and assessment of cytochrome C (cytC) oxidase activity in tissue homogenates showed a significant increase of cytC oxidase activity in s.c. adipose tissue (Fig. 7*I*). Altogether, this set of results suggests that LS condition can be associated with improved mitochondria biogenesis and/or activity, possibly through *PGC-1* up-regulation, which could explain, in part, increased energy expenditure.

LS Patients May Also Display a Lean Phenotype. Finally, we started to evaluate whether leanness and reduced adiposity found in LS mice were also a phenotypic trait of patients with LS. Clinical data were available in 28 patients with LS, genetically confirmed with a mutation in the *PTPN11* ($n = 27$) or *RAF1* ($n = 1$) genes. Most of LS patients (20 of 28 patients; 71%) had body mass index (BMI) *z* score in the lower normal range with a median *z* score of −0.6 (range −1.5–1.2) (Fig. 8*A*). This distribution was similar whatever the *PTPN11* mutations, indicating no obvious genotype/phenotype correlation, although the groups were too small to draw definite conclusions (Fig. 8*B*). Moreover, for two of these patients (BMI *z* score of −0.9 and −0.8, respectively), dual-energy X-ray absorptiometry (DXA) analysis and biochemical measurements were available. Interestingly, these case reports revealed that both patients had reduced adiposity with a percentage of fat body mass *z* score of −2.4 and −1.8 (Table 2). Consistent with this finding, both patients displayed very low levels of plasma leptin, highlighting that their reduced adiposity may have functional consequences. Thus, although preliminary, these results strongly suggest that LS condition can be associated with a lean phenotype in humans.

Discussion

In this study, we designed a mouse model carrying one mutated allele of the *Ptpn11* gene encoding the T468M mutant of SHP2 to explore the metabolic consequences of LS-associated SHP2 mutations. Extensive phenotyping of this LS mouse strain revealed that, in addition to the expected and previously observed symptoms (13, 19), LS animals exhibit markedly reduced adiposity and overall better metabolic profile, resulting in a lean and DIO resistance phenotype. Importantly, preliminary data obtained in a French

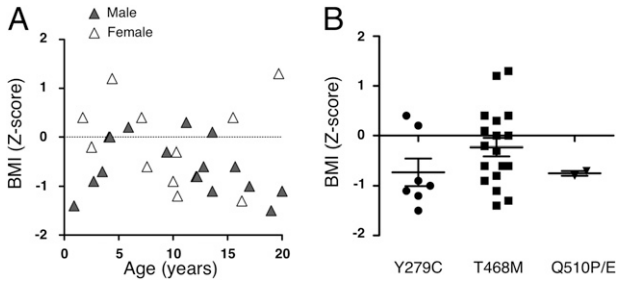

Fig. 8. Most LS patients display lower-than-average BMI. (*A*) BMI *z* score of female and male LS patients were plotted against age. (*B*) BMI *z* score of LS patients were plotted against *PTPN11* mutations.

cohort of LS patients suggest that such metabolic modifications could be found in humans; indeed, most of them display a lower-than-average BMI, which correlates, for the few patients we could test, with reduced adiposity. Altogether, our study demonstrates, for the first time to our knowledge, that LS condition can be associated with a metabolic benefit.

Beyond LS pathophysiology, our findings also highlight a key role for SHP2 in the regulation of whole body energy homeostasis. Interestingly, the positive metabolic outcomes of general expression of a LS mutant of SHP2 appear to be at odds with the few models of systemic inhibition of SHP2 function described so far. Indeed, half reduction of SHP2 expression in $SHP2^{+/-}$ mice had no impact on body weight and glucose metabolism, whereas overexpression of a dominant negative mutant in transgenic mice gave rise to glucose intolerance and insulin insensitivity (20, 21). Noticeably, none of these models has been reported to develop the clinical traits of LS. These apparent discrepancies could probably be explained by the respective amount of functional SHP2 that can be recruited to signaling complexes and transduce information. Moreover, this difference also suggests that LS mutations do not simply result in a loss-of-function effect. Indeed, it might well be that LS mutants can retain some docking, phosphatase-independent activity or could have some substrate trapping effect (16, 17).

We got first molecular insights into how LS-associated SHP2 T468M mutant can drive a lean phenotype. Indeed, we determined that expression of LS-associated SHP2 mutants in vivo and in vitro resulted in hyperactivation of both PI3K/Akt and MAPK in several metabolic tissues in response to insulin. In contrast to LS-associated PI3K/Akt hyperactivation, which has been observed in several models (13, 19), LS mutant-induced MAPK hyperactivation is more controversial. Indeed, in heart from $Ptpn11^{Y279C/+}$ mice, MAPK ERK1/2 phosphorylation was strongly reduced in response to several agonists, including insulin (13), a feature that was also found in the $Ptpn11^{T468M/+}$ mice. However, expression of LS mutants promoted MAPK hyperactivation in other biological models and in vitro, notably under basal and low stimulation conditions (14–16). One can thus imagine that LS mutants differently affect ERK1/2-regulating mechanisms depending on the cell type and on the signal nature and strength. Importantly, we provide some evidences that LS-associated leanness can be due, at least in part, to MAPK up-regulation, because chronic MEK inhibition partially reverted the lean phenotype of LS mice. In contrast, chronic treatment with rapamycin did not affect body weight and adiposity of LS mice, but strongly impaired their glucose tolerance. Interestingly, PI3K/Akt/mTOR hyperactivation has also been reported in other LS mouse models, notably in cardiac tissue following insulin injection, and has been involved in LS-associated cardiac defects (13, 19). Altogether, our results suggest that combined dysregulation of the Ras/MAPK and PI3K/Akt/mTOR pathways may participate to the lean phenotype of the LS mice. Moreover, dysregulation of additional signaling cues could certainly participate in the implementation of the metabolic phenotype in LS mice.

Going into details about the metabolic consequences of LS mutation, the most prominent feature of LS mice is their strong reduction in adiposity and their DIO resistance phenotype, which can be the resultant of several dysfunctions. First, we have shown that LS-causing mutation reduces the differentiation of SVF-derived cells into adipocytes, suggesting a defect in adipogenesis. Supporting this view, aP2-Cre–mediated *Ptpn11* invalidation in adipose tissue strongly impairs adipose tissue development, and SHP2 knockdown in a preadipocyte cell line or in pluripotent embryonic stem cells strongly inhibited adipocyte differentiation (29, 30). Defective adipogenesis could result from dysregulation of specific signaling pathways in adipocyte precursors, notably p38, as proposed by He et al. (30) or MAPK ERK1/2 (32), but also from inappropriate production of adipogenesis-regulating factors. Of note, more general determination processes might be impaired in LS mice, because SHP2 has been shown to control stem cell development (33, 34). Besides an adipogenesis defect, reduced fat mass can arise from enhanced lipolysis activity. However, the precise mechanisms that stimulate lipolysis in LS adipocytes remain to be established. Interestingly, one may hypothesize that the observed enhanced insulin-evoked MAPK activation in LS adipose tissue can sustain lipolysis, because MAPK can down-regulate perilipin and activate HSL (35, 36). Second, beyond an intrinsic effect on adipose tissue maintenance, reduced adiposity and DIO resistance of LS mice is also certainly due, at least in part, to their increased energy expenditure. Interestingly, hepatic inactivation of SHP2 (LSHKO mice) also resulted in resistance to HFD-induced obesity and increased energy expenditure (28), suggesting that reduced SHP2 activity in the liver of LS mice participates in their DIO resistance. However, because LSHKO mice have normal body weight under ND, increased energy expenditure in other organs, notably adipose tissue, may contribute to LS mice leanness (25). Supporting this view, we found that the key enhancers of mitochondriogenesis and energy metabolism *PGC-1* were overexpressed in both liver and adipose tissue of LS mice, and that mitochondrial density and cytochrome C oxidase activity were increased in some fat pads. In addition, we could determine that some markers of adipose tissue beiging were up-regulated in adipose tissues from LS mice, notably in s.c. fat pads, suggesting that this adipose tissue has enhanced oxidative activity, which could contribute to enhanced energy expenditure. Interestingly, several studies have shown that SHP2 could regulate mitochondria activity, although the signaling pathways that link SHP2, and its LS-associated mutants, to the regulation of mitochondria function and energy homeostasis remain to be documented (37–42).

Our study also highlights that T468M SHP2 mutant expression gives rise to overall better metabolic status. Indeed, LS mice display normal plasma lipid profile, under ND and HFD conditions, with only a slight reduction of cholesterol level when fed a HFD. Moreover, ectopic lipid deposits in liver and muscle were

Table 2. Case report: Clinical data from 2 LS patients (age- and sex-adapted normal range)

Clinical data	Patient 1	Patient 2
Mutation	c.1403C > T (T468M)	c.836A > G (Y279C)
Age	7	10
Sex	Female	Female
Weight, kg	18	22.8
Weight, SD	−1.00	−3.00
Height, m	1.14	1.24
Height, SD	−1.00	−2.10
BMI, kg/m^2	13.9	14.9
BMI, SD	−0.9	−0.8
% fat mass, SD	−2.4	−1.8
Leptin, mg/L	2.8 (3.7–11.1)	2.9 (3.7–11.1)

Standard deviation (SD) and normal range for leptin concentration, indicated with parentheses, are age and sex adapted.

significantly reduced in LS mice, even when fed a HFD, suggesting an improved lipid metabolism for LS mice despite reduced adiposity. Interestingly, LSHKO mice fed a HFD were also found with decreased hepatic lipid storage and serum triglycerides, suggesting that SHP2 partial inactivation in the liver of LS mice participates to this phenotype (28). Importantly, LS mice were also found with improved carbohydrates metabolism. Although reduced adiposity in LS mice may contribute to their better insulin sensitivity, our in vitro results show that expression of LS mutants is sufficient to enhance insulin signaling. Moreover, LSHKO mice also display improved glucose tolerance and insulin sensitivity, under HFD and in normal chow conditions (25, 28), suggesting that improvement of glucose metabolism in LS mice could be due to an effect of LS mutant at the hepatic level. It is also important to note that insulin levels in LS mice remained low, albeit glucose-inducible, even in aged or HFD-fed mice. Although this feature could be linked to their enhanced insulin sensitivity, expression of LS-associated SHP2 mutant in the pancreas may also inhibit insulin secretion, because it has been shown that SHP2 deletion in the pancreas strongly reduces glucose-induced insulin secretion (27).

Importantly, the lean phenotype of the LS mice appears to be at variance with several models of tissue-specific SHP2 knockouts. Indeed, SHP2 invalidation in muscle results in insulin insensitivity and glucose intolerance, with triglycerides accumulation in the muscle (26), whereas the opposite phenotype is observed in LS mice. Moreover, in contrast to LS mice that display reduced adiposity and DIO resistance, mice lacking SHP2 at the neuronal level have been shown to develop obesity and/or diabetes. Interestingly, these opposite features appear to be related to leptin signaling, because neuronal SHP2 knockout is associated with hyperleptinemia and leptin resistance (22–24), whereas LS mice display no sign of leptin resistance and low leptin level. Regarding this latter low leptinemia, it may contribute to the reduced blood pressure observed in the LS mice, because it has been demonstrated by He et al. that reduced adiposity and leptin level were causally linked to hypotension in an adipose tissue-specific SHP2 KO mouse model (30).

Altogether, these data reveal that the metabolic phenotype of LS mice is not simply the sum of the different tissue-specific models of SHP2 invalidation. A molecular explanation for this difference could be that heterozygous expression of the T468M mutant of SHP2 induces both PI3K and MAPK hyperactivation in metabolic tissues, notably in response to insulin, whereas SHP2 invalidation has different impact on these signaling pathways depending on the targeted tissue. Thus, LS mice resemble LSHKO mice, in which a strong PI3K up-regulation has been observed in the liver (25, 28), but differ from models of tissues specific to SHP2 inactivation that mainly results in MAPK inhibition (muscle, brain) (23, 26). However, because LS mutant can also inhibit the MAPK pathway, notably in cardiac tissue (13), detailed analysis of activation levels of those particular signaling pathways, in different tissues and in response to various agonists, will be necessary to validate this concept.

The identification of a lean phenotype in the LS mouse model also raises several questions in pathophysiology. First, does this apparent metabolic benefit participate in some symptoms of the disease? For instance, it is well established that an imbalance in metabolic substrate utilization, and altered response to insulin and key cardiac function regulating adipokines (e.g., leptin, adiponectin), can participate in the development of HCM, the most frequent LS-associated cardiopathy (43, 44). Therefore, it would be worthwhile to complete and extend to additional cases the metabolic exploration of LS patients, and to correlate their metabolic status to the development of other symptoms of the disease. Second, is this metabolic advantage a characteristic of SHP2 mutation-driven LS or a common feature of Rasopathies? That MAPK hyperactivation can be a cause of the lean phenotype of LS mice argues in favor of the latter. Noticeably, recent surveys have reported that patients with Rasopathies, notably with Noonan syndrome, rarely develop into being overweight or obese (45, 46). Interestingly, Wu et al. (47) have shown that PD0325901-mediated MAPK inhibition in a mouse model of Noonan syndrome caused significant increase in body weight and adiposity, suggesting a protective role of MAPK hyperactivation toward the development of obesity. Therefore, it might be important to generalize metabolic exploration to other Rasopathies. Last but not least, because heterozygous expression of an LS mutant of SHP2 enhances energetic metabolism and has a protective effect toward obesity and diabetes, one may wonder whether equivalent pharmacological modulation of SHP2, that functionally mimics LS mutations, could be a potent strategy to alleviate obesity and associated pathologies. Indeed, it has been shown that SHP2 expression is up-regulated in metabolic tissues from obese animals, suggesting that increased SHP2 expression/activity contributes to the development of obesity (28, 31, 48, 49). Further studies are definitely warranted to address these burning questions.

Materials and Methods

Mouse Studies. All procedures were performed in accordance with institutional guidelines for animal research and were approved by the Animal Care and Use Committee of Institut National de la Santé et de la Recherche Médicale US006. For all in vivo studies, male mice *Ptpn11*$^{T468M/+}$ and their *Ptpn11*$^{+/+}$ littermates have been compared. For reversion experiments, animals were injected i.p. with 1 mg·kg^{-1}·d^{-1} PD0325901, 2 mg·kg^{-1}·d^{-1} rapamycin or vehicle as a control for 1 mo. EchoMRI analyses (Echo Medical Systems) were performed by following manufacturer's instructions to determine body composition. For OGTT and ITT, after 6-h fasting, mice were fed with glucose (3 g/kg) for OGTT or injected with insulin (0.5 units/kg) for ITT, then blood was taken from the tail vein and glucose levels were monitored over time by using a glucometer (Accu-check; Roche Diagnostics) or using Glucose RTU kit (bioMérieux). Indirect calorimetry was performed at the indicated age after 24 h of acclimatization in individual cages. O_2 consumption (VO_2) and CO_2 production (VCO_2) were measured (Oxylet; Panlab-Bioseb) in individual mice at 25-min intervals during a 24-h period. The respiratory quotient (RQ = VCO_2/VO_2) and energy expenditure (in kcal·d^{-1}·kg^{-1}, $0.75 = 1.44 \times VO_2 \times [3.815 + 1.232 \times RQ]$) were calculated. Ambulatory activities of the mice were monitored by an infrared photocell beam interruption method (Sedacom; Panlab-Bioseb).

Lentiviral Transduction and Insulin Stimulation of Mouse Embryonic Fibroblasts. Previously described cDNA encoding V5-SHP2-WT, T468M, and –Y279C (18) were made shRNA-resistant by generating silent mutations through site-directed mutagenesis, then subcloned into the previously described pLVTHM/sh-SHP2 in lieu of the GFP cassette (50). Lentivectors were generated as described in ref. 50 and used to transduce immortalized MEFs. Cells were seeded in 60-mm dishes, serum deprived, then stimulated or not with 50 nM insulin for 5 min, rinsed with ice cold PBS, lysed in Laemmli's sample buffer, and processed for Western blot analysis.

Clinical Data Collection and Analysis. The data collection and exploration of genes for LS patients was performed in the Department of Genetics, Assistance Publique-Hôpitaux de Paris-Robert Debré Hospital, Paris, and was approved by Institutional Review Boards (Program Hospitalier de Recherche Clinique National, AOM02004). Written informed consent was obtained from the legal guardians and/or patients. Auxological data (height and weight) were available in 28 patients (11 females, 17 males, age range 0–20 y old). BMI was calculated as the ratio of weight in kilograms divided by the square of height in meters, and BMI measurements were converted to age- and sex-specific *z* scores on the basis of French reference data (51). Fat body mass was measured by dual-energy X-ray absorptiometry (DXA) analysis by using a Lunar Prodigy device (GE Healthcare), expressed as a percentage of total body mass and transformed to age-specific *z* scores (52).

Statistics. All data are expressed as mean ± SEM. Except otherwise indicated, statistical significance was determined by using paired or unpaired two-tailed Student *t* test, with Welch correction in case of unequal variances, two-way ANOVA with Bonferroni post hoc test, or two-way ANOVA with repeated measures, as appropriate. *P* values <0.05 were considered significant (*$P < 0.05$; **$P < 0.01$; ***$P < 0.001$).

ACKNOWLEDGMENTS. We thank the Mouse Clinical Institute for generation of the *Ptpn11*$^{T468M/+}$ mice; the personnel of the Anexplo animal facilities for animal handling; the Phenotyping platform and the Non-Invasive Exploration service –US006/Centre Régional d'Exploration Fonctionnelle et de

Ressources Expérimentales Institut National de la Santé et de la Recherche Médicale (INSERM)/Université Paul Sabatier; the histology facility of Unité Mixte de Recherche U1048; all past and present members of the Adipolab for technical and scientific support; Drs. C. Dray, J-S. Saulnier-Blache, I. Castan-Laurell, C. Bertrand, and C. Rancoule for fruitful discussions and technical assistance; and L. Casteilla, A. Galinier, A. Carrière, and D. Langin for invaluable advice. This work was supported by grants from INSERM, Ministère de l'Education Nationale de la Recherche et de la Technologie (France), Groupement d'Intérêt Scientifique-Maladies Rares, Agence Nationale de la Recherche, e-Rare (European Network on Noonan syndrome and related disorders, NSEuroNet), Institut National du Cancer and Direction de l'Hospitalisation et de l'Offre de Soins/INSERM.

1. Tartaglia M, Gelb BD, Zenker M (2011) Noonan syndrome and clinically related disorders. *Best Pract Res Clin Endocrinol Metab* 25(1):161–179.
2. Keren B, et al.; French Collaborative Noonan Study Group (2004) PTPN11 mutations in patients with LEOPARD syndrome: A French multicentric experience. *J Med Genet* 41(11):e117.
3. Grossmann KS, Rosário M, Birchmeier C, Birchmeier W (2010) The tyrosine phosphatase Shp2 in development and cancer. *Adv Cancer Res* 106:53–89.
4. Zhang SQ, et al. (2002) Receptor-specific regulation of phosphatidylinositol 3′-kinase activation by the protein tyrosine phosphatase Shp2. *Mol Cell Biol* 22(12):4062–4072.
5. Zhang SQ, et al. (2004) Shp2 regulates SRC family kinase activity and Ras/Erk activation by controlling Csk recruitment. *Mol Cell* 13(3):341–355.
6. Chen Y, et al. (2003) Identification of Shp-2 as a Stat5A phosphatase. *J Biol Chem* 278(19):16520–16527.
7. Dance M, Montagner A, Salles JP, Yart A, Raynal P (2008) The molecular functions of Shp2 in the Ras/Mitogen-activated protein kinase (ERK1/2) pathway. *Cell Signal* 20(3):453–459.
8. Zito CI, Qin H, Blenis J, Bennett AM (2007) SHP-2 regulates cell growth by controlling the mTOR/S6 kinase 1 pathway. *J Biol Chem* 282(10):6946–6953.
9. Kontaridis MI, et al. (2004) SHP-2 positively regulates myogenesis by coupling to the Rho GTPase signaling pathway. *Mol Cell Biol* 24(12):5340–5352.
10. Hanna N, et al. (2006) Reduced phosphatase activity of SHP-2 in LEOPARD syndrome: Consequences for PI3K binding on Gab1. *FEBS Lett* 580(10):2477–2482.
11. Tartaglia M, et al. (2006) Diversity and functional consequences of germline and somatic PTPN11 mutations in human disease. *Am J Hum Genet* 78(2):279–290.
12. Kontaridis MI, Swanson KD, David FS, Barford D, Neel BG (2006) PTPN11 (Shp2) mutations in LEOPARD syndrome have dominant negative, not activating, effects. *J Biol Chem* 281(10):6785–6792.
13. Marin TM, et al. (2011) Rapamycin reverses hypertrophic cardiomyopathy in a mouse model of LEOPARD syndrome-associated PTPN11 mutation. *J Clin Invest* 121(3):1026–1043.
14. Oishi K, et al. (2009) Phosphatase-defective LEOPARD syndrome mutations in PTPN11 gene have gain-of-function effects during Drosophila development. *Hum Mol Genet* 18(1):193–201.
15. Carvajal-Vergara X, et al. (2010) Patient-specific induced pluripotent stem-cell-derived models of LEOPARD syndrome. *Nature* 465(7299):808–812.
16. Yu ZH, et al. (2013) Structural and mechanistic insights into LEOPARD syndrome-associated SHP2 mutations. *J Biol Chem* 288(15):10472–10482.
17. Stewart RA, et al. (2010) Phosphatase-dependent and -independent functions of Shp2 in neural crest cells underlie LEOPARD syndrome pathogenesis. *Dev Cell* 18(5):750–762.
18. Edouard T, et al. (2010) Functional effects of PTPN11 (SHP2) mutations causing LEOPARD syndrome on epidermal growth factor-induced phosphoinositide 3-kinase/AKT/glycogen synthase kinase 3beta signaling. *Mol Cell Biol* 30(10):2498–2507.
19. Schramm C, Fine DM, Edwards MA, Reeb AN, Krenz M (2012) The PTPN11 loss-of-function mutation Q510E-Shp2 causes hypertrophic cardiomyopathy by dysregulating mTOR signaling. *Am J Physiol Heart Circ Physiol* 302(1):H231–H243.
20. Arrandale JM, et al. (1996) Insulin signaling in mice expressing reduced levels of Syp. *J Biol Chem* 271(35):21353–21358.
21. Maegawa H, et al. (1999) Expression of a dominant negative SHP-2 in transgenic mice induces insulin resistance. *J Biol Chem* 274(42):30236–30243.
22. Zhang EE, Chapeau E, Hagihara K, Feng GS (2004) Neuronal Shp2 tyrosine phosphatase controls energy balance and metabolism. *Proc Natl Acad Sci USA* 101(45):16064–16069.
23. Krajewska M, et al. (2008) Development of diabesity in mice with neuronal deletion of Shp2 tyrosine phosphatase. *Am J Pathol* 172(5):1312–1324.
24. Banno R, et al. (2010) PTP1B and SHP2 in POMC neurons reciprocally regulate energy balance in mice. *J Clin Invest* 120(3):720–734.
25. Matsuo K, et al. (2010) Altered glucose homeostasis in mice with liver-specific deletion of Src homology phosphatase 2. *J Biol Chem* 285(51):39750–39758.
26. Princen F, et al. (2009) Deletion of Shp2 tyrosine phosphatase in muscle leads to dilated cardiomyopathy, insulin resistance, and premature death. *Mol Cell Biol* 29(2):378–388.
27. Zhang SS, et al. (2009) Coordinated regulation by Shp2 tyrosine phosphatase of signaling events controlling insulin biosynthesis in pancreatic beta-cells. *Proc Natl Acad Sci USA* 106(18):7531–7536.
28. Nagata N, et al. (2012) Hepatic Src homology phosphatase 2 regulates energy balance in mice. *Endocrinology* 153(7):3158–3169.
29. Uehara T, et al. (2007) SHP-2 positively regulates adipogenic differentiation in 3T3-L1 cells. *Int J Mol Med* 19(6):895–900.
30. He Z, et al. (2013) Nonreceptor tyrosine phosphatase Shp2 promotes adipogenesis through inhibition of p38 MAP kinase. *Proc Natl Acad Sci USA* 110(1):E79–E88.
31. Bettaieb A, et al. (2011) Adipose-specific deletion of Src homology phosphatase 2 does not significantly alter systemic glucose homeostasis. *Metabolism* 60(8):1193–1201.
32. Gehart H, Kumpf S, Ittner A, Ricci R (2010) MAPK signalling in cellular metabolism: Stress or wellness? *EMBO Rep* 11(11):834–840.
33. Wu D, et al. (2009) A conserved mechanism for control of human and mouse embryonic stem cell pluripotency and differentiation by shp2 tyrosine phosphatase. *PLoS ONE* 4(3):e4914.
34. Feng GS (2007) Shp2-mediated molecular signaling in control of embryonic stem cell self-renewal and differentiation. *Cell Res* 17(1):37–41.
35. Liu LR, et al. (2011) Serum amyloid A induces lipolysis by downregulating perilipin through ERK1/2 and PKA signaling pathways. *Obesity (Silver Spring)* 19(12):2301–2309.
36. Greenberg AS, et al. (2001) Stimulation of lipolysis and hormone-sensitive lipase via the extracellular signal-regulated kinase pathway. *J Biol Chem* 276(48):45456–45461.
37. Salvi M, et al. (2004) Tyrosine phosphatase activity in mitochondria: Presence of Shp-2 phosphatase in mitochondria. *Cell Mol Life Sci* 61(18):2393–2404.
38. Arachiche A, et al. (2008) Localization of PTP-1B, SHP-2, and Src exclusively in rat brain mitochondria and functional consequences. *J Biol Chem* 283(36):24406–24411.
39. Duarte A, et al. (2012) Mitochondrial fusion is essential for steroid biosynthesis. *PLoS ONE* 7(9):e45829.
40. Lee I, et al. (2010) A suggested role for mitochondria in Noonan syndrome. *Biochim Biophys Acta* 1802(2):275–283.
41. Xu D, Zheng H, Yu WM, Qu CK (2013) Activating mutations in protein tyrosine phosphatase Ptpn11 (Shp2) enhance reactive oxygen species production that contributes to myeloproliferative disorder. *PLoS ONE* 8(5):e63152.
42. Zheng H, Li S, Hsu P, Qu CK (2013) Induction of a tumor-associated activating mutation in protein tyrosine phosphatase Ptpn11 (Shp2) enhances mitochondrial metabolism, leading to oxidative stress and senescence. *J Biol Chem* 288(36):25727–25738.
43. Cornier MA, Marshall JA, Hill JO, Maahs DM, Eckel RH (2011) Prevention of overweight/obesity as a strategy to optimize cardiovascular health. *Circulation* 124(7):840–850.
44. Abel ED, Litwin SE, Sweeney G (2008) Cardiac remodeling in obesity. *Physiol Rev* 88(2):389–419.
45. Binder G, et al. (2012) Health and quality of life in adults with Noonan syndrome. *J Pediatr* 161(3):501–505, e1.
46. Malaquias AC, et al. (2012) Growth standards of patients with Noonan and Noonan-like syndromes with mutations in the RAS/MAPK pathway. *Am J Med Genet A* 158A(11):2700–2706.
47. Wu X, et al. (2011) MEK-ERK pathway modulation ameliorates disease phenotypes in a mouse model of Noonan syndrome associated with the Raf1(L613V) mutation. *J Clin Invest* 121(3):1009–1025.
48. Tagami S, et al. (2002) Troglitazone ameliorates abnormal activity of protein tyrosine phosphatase in adipose tissues of Otsuka Long-Evans Tokushima Fatty rats. *Tohoku J Exp Med* 197(3):169–181.
49. Ahmad F, Goldstein BJ (1995) Alterations in specific protein-tyrosine phosphatases accompany insulin resistance of streptozotocin diabetes. *Am J Physiol* 268(5 Pt 1):E932–E940.
50. De Rocca Serra-Nédélec A, et al. (2012) Noonan syndrome-causing SHP2 mutants inhibit insulin-like growth factor 1 release via growth hormone-induced ERK hyperactivation, which contributes to short stature. *Proc Natl Acad Sci USA* 109(11):4257–4262.
51. Rolland-Cachera MF, et al. (1991) Body Mass Index variations: Centiles from birth to 87 years. *Eur J Clin Nutr* 45(1):13–21.
52. van der Sluis IM, de Ridder MA, Boot AM, Krenning EP, de Muinck Keizer-Schrama SM (2002) Reference data for bone density and body composition measured with dual energy x ray absorptiometry in white children and young adults. *Arch Dis Child* 87(4):341–347, discussion 341–347.